京都大学防災研究所年報 第 54 号 B 平成 23 年 6 月
Annuals of Disas. Prev. Res. Inst., Kyoto Univ., No. 54 B, 2011

Erosion Characteristics of Cohesive Sediment by Non-Cohesive Sediment

Puji HARSANTO, Nguyen Manh Minh TOAN*, Hiroshi TAKEBAYASHI and Masaharu FUJITA

* Graduate School of Engineering, Kyoto University

Synopsis

The purpose of this paper is to study the erosion characteristics of cohesive sediment by both non-cohesive sediment and clear water. The results of flume experiment and the dynamic shear stress on the bed are discussed. The flume experiments were conducted with non-cohesive sediment is supplied on the cohesive sediment. The transport rate of the non-cohesive sediment supply is varied from 0 to 150% of the equilibrium sediment transport rate. The results indicate that, when bed is composed of 100% cohesive sediment, the bed degradation depth with sediment supply are more than without sediment supply or in clear water and the erosion rate is decreased with increase in sediment discharge. Because the dynamic shear stress on the bed is decreased with increase in sediment discharge.

Keywords: cohesive sediment, erosion rate, sediment feeding rate, non-cohesive material, dynamic shear stress

1. Introduction

Cohesive sediment is a mixture of clay particles, silt, (fine) sand, organic material and so on. The cohesive properties arise from electrochemical forces in the clay-water medium. These forces usually dominate and larger than the weight force of individual particles (Raudkivi, 1990). Fig. 1 shows the bank of the Mekong River in Vietnam. Some layers of the bank material are composed of cohesive material. As shown in Fig. 1, we can easy to find the deposition layer of cohesive sediment in natural rivers. Hence, in order to understand the channel and bed deformation phenomena, erosion rate of cohesive sediment has been investigated by many researchers.

Laboratory and in situ experimental have been conducted by many researchers (e.g. Parchure and Mehta, 1985; Chapalain et al., 1994; Roberts et al., 1998; Sekine and Iizuka, 2000; Aberle et al., 2002).

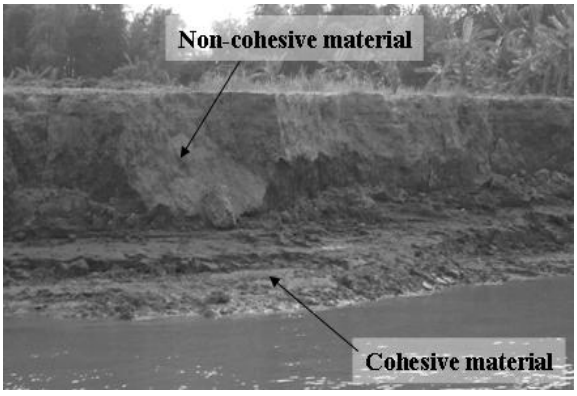

Fig. 1 A river with bed composed of both cohesive and non-cohesive materials at The Mekong River, Vietnam (Takebayashi et al., 2005)

Most of them focused on temperature of water, water content of the cohesive material, bulk density, etc. to study on erosion rate of cohesive sediment by clear water. As most formulas of erosion rate of cohesive sediment have a similar form on relation

between the erosion rate and the bed shear stress, and erosion rate increases with the increase in bed shear stress. Those researches give us important knowledge to understand erosion characteristics of cohesive sediment.

By the way, bed material in river is non-uniform sediment. And non-cohesive coarse material and cohesive material coexist in rivers. For example, the coarse non-cohesive material in the Mekong River flows on the fine cohesive material in the Tonle Sap River during the flood season around Phnom Penh in Cambodia (Takebayashi et al., 2005). This fact indicates that the cohesive material can be eroded by both non-cohesive material and water.

The influence of coarse material sediment on cohesive sediment erosion is presented in (Kamphius, 1999). The results indicate that the presence of granular material on erosion of cohesive sediment is very important. Erosion was most rapid when the sand moving by saltation and decreased if the sand either moved as pure bedload which covered the bed at certain times. Thus erosion rate is a function of fluid velocities and turbulence, as well as sediment concentrations. From this results give knowledge that the size and volume of non-cohesive sediment is important matter for erosion process of cohesive sediment.

In this study, the erosion characteristics of cohesive sediment by both non-cohesive sediment and clear water are discussed with consider of volume and granular sediment size. Flume tests are performed under various sediment supply conditions. Furthermore, the dynamic shear stress on bed is calculated considering the vertical distribution of longitudinal velocity and sediment concentration and discussed the erosion rate of the cohesive material by both water and non-cohesive coarse material.

2. Flume test

2.1 Experimental setup

Experimental setup is shown in Fig. 2. The experiments were carried out in the flume with 800 cm long, 15 cm wide and 25 cm deep. The base cohesive sediment used in this study was prepared from dry kaolin powder.

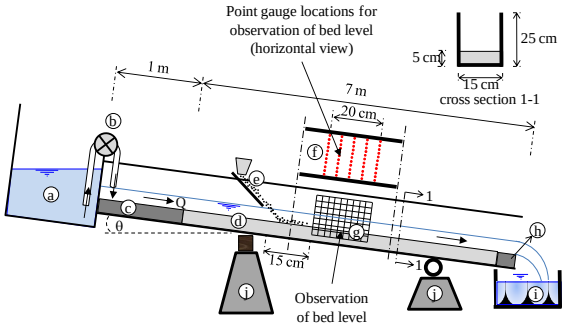

Fig. 2 The experiment setup, where a) water tank, b) pump, c) rigid bed, d) cohesive sediment, e) sediment feeding location, f) horizontal view of cross sections, g) screen grid, h) downstream weir, i) downstream tank, and j) tilting machine)

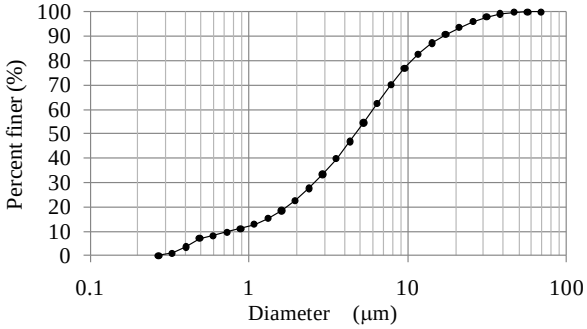

Fig. 3 Grain size distribution of cohesive material

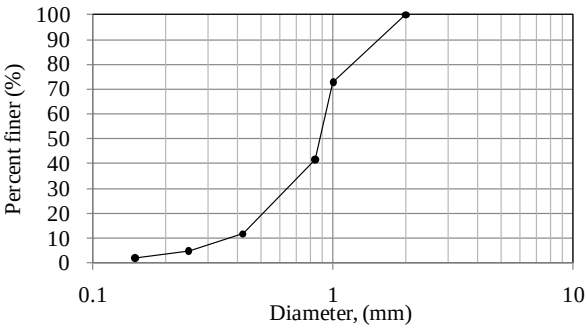

Fig. 4 Grain size distribution of non-cohesive

Fig. 3 shows the grain size distribution of the dry kaolin powder that used in this experiment as material for cohesive sediment. The grain size of this material is between 0.328 μm and 68.973 μm with d_{50} is 4.616 μm. Two types of cohesive sediment are used in the experiment. Type A is the cohesive sediment which is composed of 100% cohesive material. Type B is the cohesive sediment which is composed of 50% cohesive material and 50% coarse sand. Fig. 4 shows the grain size distribution of coarse sand (non-cohesive material). Specific gravity of non-cohesive material is 2.65 and mean diameter is 0.88 mm. The cohesive sediment was laid on the bed with 700 cm long, 15

cm width and 5 cm thickness. The water content was designed around 50% for Type A and 30% for Type B. To prepare the cohesive sediment, the cohesive materials and water were put into a bucket and were mixed until the sample became mud that has homogeneous condition. After this preparation, the sample is put in the flume experiment and pooled by water. The cohesive materials have been kept in the pooled channel for one day in order to allow for settling and consolidation naturally. During settling and consolidation process, the bed geometry is kept in flat condition.

2.2 Measurement method

In order to evaluate the bed elevation change on the surface of cohesive sediment, bed elevations before and after experiment were measured. Bed levels were measured at 11 places in a cross section and 5 cross sections are measured. The longitudinal step between the cross sections is 5 cm. Bed elevation change is also monitored during experiments by use of a digital high speed camera from the side wall of the flume. Video camera was shot on acrylic wall, which has grids on it as shown in Fig. 5.

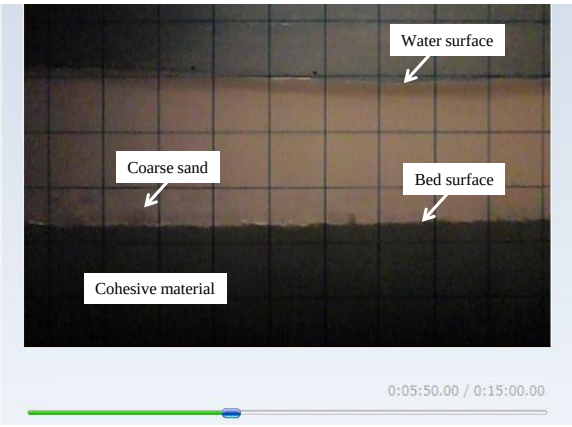

Fig. 5 Example of snap shot by the high speed video camera

Water velocity on the water surface was measured by floating material tracking method. One more digital high speed camera was placed above of water surface. The transparence grid was placed between video camera and water surface. Neutral particles were put from the upstream of flume during experiment. Water level was measured longitudinally along the center line of the flume. Water level also measured by digital high speed camera from the side wall of flume as shown in Fig. 5. Water temperature and water content also measure at every experiment. Water content of cohesive sediment was measured after experiments by taking the sample from the bed.

2.3 Hydraulics condition

The hydraulic conditions of the experiments are shown in Table 1. The aim of these experiments was clarified the effect of sediment discharge of non-cohesive coarse sediment on the erosion rate of cohesive sediment. In order to produce sediment transport of non-cohesive coarse sediment, non-cohesive coarse sediment was fed from the upstream of the flume during the experiments. The supplied sediment is the same as the coarse sand which is used in Type B. Fig. 4 shows the grain size distribution of the supplied sediment. Supplied sediment discharge is widely distributed from 0 to 1.5 times as equilibrium sediment transport rate. The temperature of the water in all cases was about 30 degree centigrade.

3. Analysis of dynamic shear stress on bed

The dynamic shear stress on bed is calculated to discuss the erosion rate of the cohesive material by both water and non-cohesive material. Two layer flows under the normal flow conditions is considered here. Water flow where Reynolds stress is dominant is assumed in the upper flow layer and laminar flow of both sediment and water is assumed in the lower flow layer. Shear stress τ and pressure p in the upper flow layer ($h_s \le z \le h_t$) are as follows:

$$\tau = \int_z^{h_t} \rho g \sin\theta dz \tag{1}$$

$$p = \int_z^{h_t} \rho g \cos\theta dz \tag{2}$$

Where, z is the vertical axis, h_t is the total flow depth, h_s is the flow depth of the lower layer, ρ is the density of water, g is the gravity acceleration, θ is the channel slope. Shear stress τ and pressure p in the lower flow layer ($0 \le z \le h_s$) are as follows, (Ashida et al., 1982):

Table 1 Case and hydraulics condition of the experiments

No.	Case	Bed material	Sediment feeding	Slope	Discharge
			(gr/s)	(m/m)	(l/s)
1	case 1	100 % cohesive	0 % q_{bp}	0.004	1.3
2	case 2	100 % cohesive	25 % q_{bp}		
3	case 3	100 % cohesive	50 % q_{bp}		
4	case 4	100 % cohesive	100 % q_{bp}		
5	case 5	100 % cohesive	150 % q_{bp}		
6	case 1a	50 % cohesive and 50% non-cohesive	0 % q_{bp}		
7	case 2a	50 % cohesive and 50% non-cohesive	25 % q_{bp}		
8	case 3a	50 % cohesive and 50% non-cohesive	50 % q_{bp}		
9	case 4a	50 % cohesive and 50% non-cohesive	100 % q_{bp}		
10	case 5a	50 % cohesive and 50% non-cohesive	150 % q_{bp}		

$$\tau = \tau_s + \tau_d + \tau_f = \int_z^{h_t} \rho_m g \sin\theta dz \quad (3)$$

$$p = p_s + p_d + p_f = \int_z^{h_s} (\sigma - \rho) cg \cos\theta dz \quad (4)$$

Where, τ_s and p_s are the shear stress and the pressure due to the static intergranular contact, respectively, τ_d and p_d are the shear stress and the pressure due to interparticle collisions, respectively, and τ_f and p_f are the shear stress and the pressure supported by the interstitial liquid phase, ρ_m is the density of mixed material of sediment and water. The constitutive equations proposed by Egashira et al. (1997) are as follows:

$$\tau_s = p_s \tan\phi_s \quad (5)$$

$$\tau_d = k_d (1 - e^2) \sigma d^2 c^{1/3} \left(\frac{\partial u}{\partial z} \right)^2 \quad (6)$$

$$\tau_f = \rho k_f d^2 \frac{(1-c)^{5/3}}{c^{2/3}} \left(\frac{\partial u}{\partial z} \right)^2 \quad (7)$$

$$p_s = \left(\frac{c}{c_*} \right)^{1/5} (p_s + p_d) \quad (8)$$

$$p_d = k_d \sigma e^2 d^2 c^{1/3} \left(\frac{\partial u}{\partial z} \right)^2 \quad (9)$$

Where, ϕ_s is the friction angle, e is the restitution coefficient, c is the volumetric sediment concentration and c_* is the volumetric sediment concentration in stationary state, σ is the density of sediment, u is the longitudinal flow velocity, k_d (=0.0828) and k_f (=0.16) are the empirical constants.

Equations 5 to 9 are substituted to equations 3 and 4 and following velocity and sediment concentration profiles are obtained.

$$(h_t - z) \frac{\partial F}{\partial z} = F - c \quad (10)$$

$$\frac{\partial u}{\partial z} = \frac{1}{d} \sqrt{\frac{g(G-Y)}{f_d + f_f}} \quad (11)$$

Where, d is the mean diameter of sediment. F, G, Y, f_d and f_f are as follows.

$$F = \frac{f_{pd} \tan\theta}{(\sigma/\rho - 1)(F_1 - F_2)} \quad (12)$$

$$G = \sin\theta \int_z^{h_s} (\sigma/\rho - 1) c dz + \sin\theta \int_z^1 dz \quad (13)$$

$$Y = \left(\frac{c}{c_*} \right)^{1/5} \cos\theta \tan\phi \int_z^{h_s} (\sigma/\rho - 1) c dz \quad (14)$$

$$f_d = k_d (1 - e^2)(\sigma/\rho) c^{1/3} \quad (15)$$

$$f_f = k_f (1-c)^{5/3} / c^{2/3} \quad (16)$$

$$f_{pd} = k_d e^2 (\sigma/\rho) c^{1/3} \quad (17)$$

$$F_1 = f_f + f_d - f_{pd} \tan\theta \quad (18)$$

$$F_2 = \left(\frac{c}{c_*} \right)^{1/5} (f_f + f_d - f_{pd} \tan\phi_s) \quad (19)$$

Logarithmic velocity profile is applied to the upper flow layer as follows:

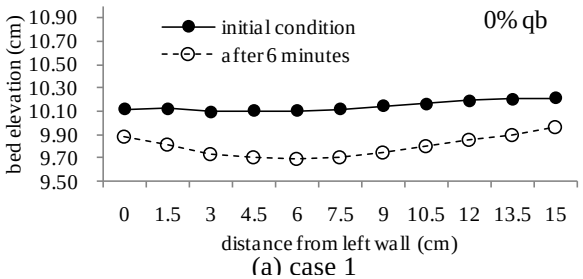

(a) case 1

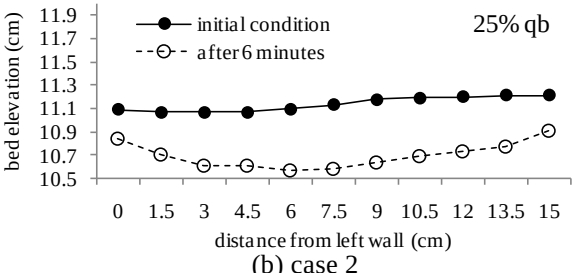

(b) case 2

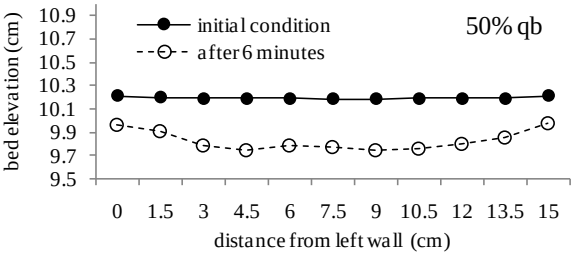

(c) case 3

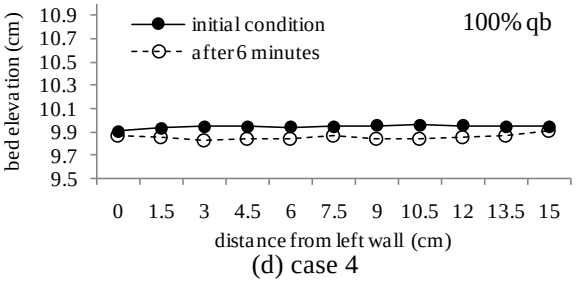

(d) case 4

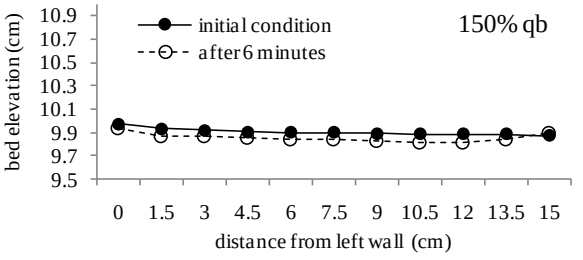

(e) case 5

Fig. 6 Bed cross section on case1 to case 5

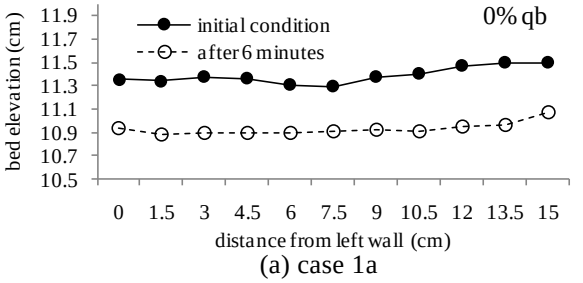

(a) case 1a

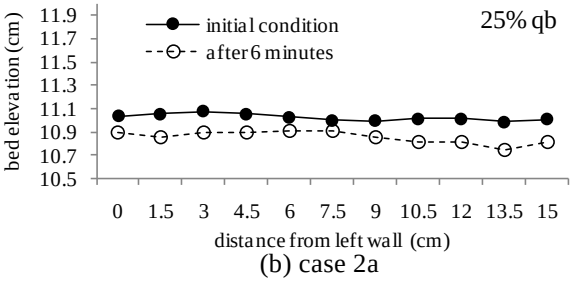

(b) case 2a

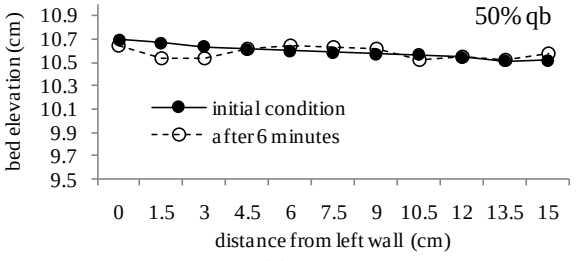

(c) case 3a

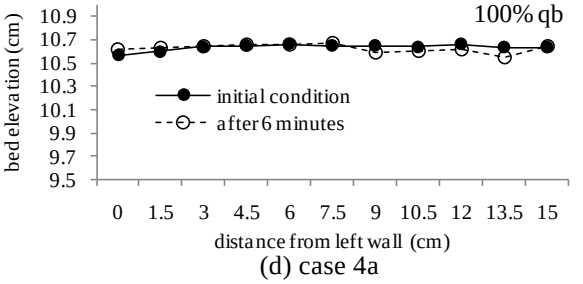

(d) case 4a

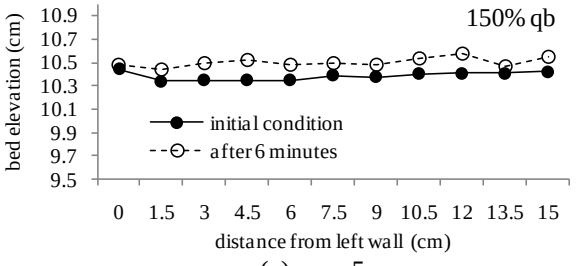

(e) case 5a

Fig. 7 Bed cross section on case 1a to case 5a

$$\frac{u}{u_*} = \frac{u_i}{u_*} + \frac{1}{\kappa}\ln\left(\frac{z - h_s + \eta_0}{\eta_0}\right) \qquad (20)$$

Where, $u_* = \sqrt{g h_w \sin\theta}$, u_i is the velocity at the interface, κ is the Karman constant, h_w is the depth of the upper flow layer. η_0 is the particle interstitial scale and estimated as follows:

$$\eta_0 = a\sqrt{k_f}\left(\frac{1-c}{c}\right)^{1/3} d \quad (a \cong 1.0) \qquad (21)$$

The height at c=0.05 is assumed for the interface height between the upper flow and the lower flow. Water velocity between the upper flow layer and the lower flow layer is connected at the interface.

The dynamic shear stress τ_{dy} is calculated by use of the following equation

$$\tau_{dy} = \tau - \tau_s \tag{22}$$

4. Results and discussions

Fig. 6 and Fig. 7 show the cross section profiles of bed. Fig. 6 (a) - (e) are the results from case 1 to case 5 (cohesive sediment type A), respectively. The effect of sediment discharge is compared between the cross section profiles. The average bed degradation depth for case 1, 2, 3, 4, and 5 after 6 minutes are 0.34 cm, 0.44 cm, 0.37 cm, 0.09 cm, and 0.05 cm, respectively. First, from Fig. 6 (a), (b) and (c), bed degradation depth with sediment supply are more than that without sediment supply. This result shows that the bed composed of the cohesive sediment will be eroded more by the addition of the coarse non-uniform sediment in the flow under some hydraulic conditions. On the other hand, Fig. 6 (d) and (e) show the bed degradation depth is smaller than that in Fig. 6 (a), (b) and (c). The maximum erosion rate is appeared at around 25% of the equilibrium sediment transport rate and the erosion rate is decreased with increase in sediment discharge. This phenomenon is discussed by use of the analysis in Chapter 3. Fig. 8 shows the vertical distribution of the longitudinal velocity, the sediment concentration and the dynamic shear stress in cases 2, 3 and 4. When sediment feeding rate is equal to the equilibrium sediment transport rate, the thickness of the bed load layer becomes maximum and velocity near bed is smaller than other two cases. The dynamic shear stress on the bed is equal to zero. Hence, the erosion rate of the cohesive material is equal to zero in the calculation. On the other hand, when sediment feeding rate is equal to 0.25 times as the equilibrium sediment transport rate, the thickness of the bed load layer becomes thin and velocity near bed is larger than other two cases. The dynamic shear stress on the bed is also larger than the other two cases. Hence, it is considered that the erosion rate of the cohesive material becomes largest among the three cases. Here, the vertical velocity of the sediment is neglected in the calculation. It must affect on the erosion rate of the

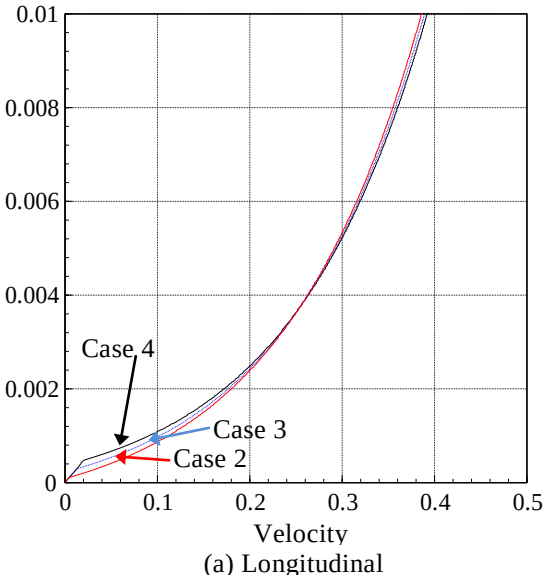

(a) Longitudinal

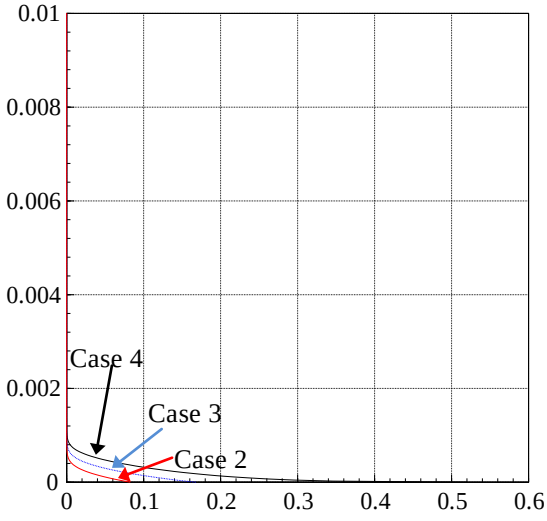

(b) Sediment

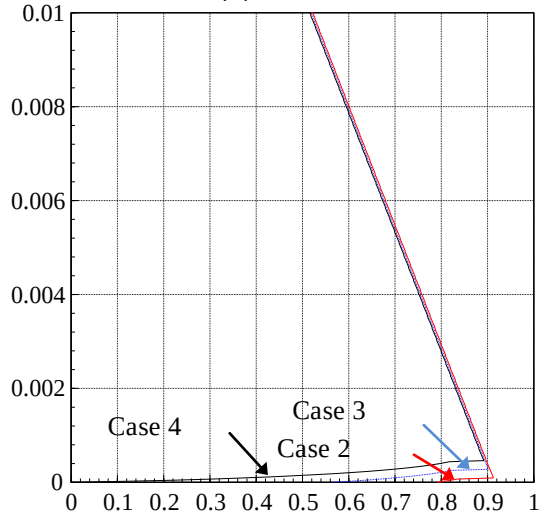

(c) Dynamic shear

Fig. 8 The vertical distribution of longitudinal velocity, sediment concentration and dynamic shear stress

cohesive material when the sediment concentration is low. It is considered that the erosion in case 3 (the equilibrium sediment transport rate) is due to this assumption.

Fig. 7 (a) - (e) are the results from case 1a to case 5a (cohesive sediment type B), respectively. The average bed changes level for cases 1a, 2a, 3a, 4a, and 5a after 6 minutes are 0.46 cm, 0.17 cm, 0.01 cm, 0.01 cm, and -0.12 cm, respectively. Here, a positive value indicates erosion and a negative value indicates deposition. The erosion rate in case 1a (without sediment supply) is the maximum among the 5 cases. Sediment supply due to the bed erosion between the upstream end of cohesive material layer and the measurement location affects on the result. In case 1a, coarse material is supplied from the bed with the bed degradation between the upstream end of cohesive material layer and the measurement location. Hence, the effect of the erosion by non-cohesive material is introduced in case 1a (without sediment supply). However, the non-equilibrium characteristics of coarse material in cohesive material are strong. Hence, it is considered that the distance from the upstream end of cohesive material layer and the measurement location, which is 4 m, is not enough to get the equilibrium sediment transport rate. As a result, the sediment transport rate at the measurement location in case 1a is close to the sediment transport rate in case 2 and the erosion rate in case1a is larger than case 1. Furthermore, erosion rate of the cohesive material decrease with increase in the sediment supply. This tendency is the same as cases 2, 3, 4 and 5.

In the natural rivers, when the bed material is composed of both cohesive material and non-cohesive coarse material like Type B, bed erosion is large in the non-equilibrium region of the sediment transport rate of non-cohesive material. However, bed will not be eroded in the equilibrium region where can be appear at the downstream of the non-equilibrium region.

5. Conclusions

The erosion characteristics of cohesive sediment by both non-cohesive sediment and clear water are discussed by use of the flume tests and the dynamic shear stress on the bed. Obtained results are summarized as follows.

[1] When bed is composed of 100% cohesive material, the bed degradation depth with sediment supply is more than that without sediment supply.

[2] When bed is composed of 100% cohesive material, the erosion rate is decreased with increase in sediment discharge. Because the dynamic shear stress on the bed is decreased with increase in sediment discharge.

[3] The erosion rate without sediment supply on bed composed of 50% cohesive material and 50% coarse sand is larger than that with sediment supply. Because coarse sand is supplied from the eroded bed in the upstream area and the non-equilibrium characteristics of coarse material in cohesive material is strong.

[4] On case which bed is composed of 50% cohesive material and 50% coarse sand, the erosion rate of the cohesive material decrease with increase of sediment supply. This tendency is the same as the cases with bed composed of 100% cohesive material.

Acknowledgements

This work is funded by Grant-in-Aid for Scientific Research (A) (Representative: Yasuyuki Shimizu), Grant-in-Aid for Scientific Research for young researchers (B) (Representative: Hiroshi Takebayashi), RIC Research Fund (Representative: Hiroshi Takebayashi), STC Research Fund (Representative: Hiroshi Takebayashi), River Fund by Foundation of River & Watershed Environment Management (Representative: Hiroshi Takebayashi).

References

Aberle, J., Nikora, V., and Walters, R. (2002): In situ measurement of cohesive sediment dynamics using a straight benthic flume-Hydraulic Measurements and Experimental Methods Conference, Estes Park, Colorado.

Ashida, K., Egashira, S., and Kamoto (1982): Study on the erosion and variation of mountain streams -On the erosion and transportation of sand-clay mixtures, Bulletine of DPRI, Kyoto University,

Vol. 25, B-2, pp. 349-360.
Chapalain, G., Sheng YP., and Temperville AT. (1994): About the specification of erosion flux for soft stratified cohesive sediments.
Egashira, S., Miyamoto, K., and Itoh, T. (1997): Constitutive equations of debris flow and their applicability, Proc. 1st Int. Conf. on Debris-Flow Hazards Mitigation, New York: ASCE: pp.340-349.
Kamphuis, J.W. (1999): Influence of sand or gravel on the erosion of cohesive sediment, Journal of Hydraulic Research, IAHR, Vol. 28-1, pp. 43-53.
Parchure, TM., and Mehta, AJ. (1985): Erosion of cohesive sediment deposits, Journal of Hydraulic Engineering, ASCE, Vol. 111, No.10, ISSN 0733-9429/85/0010-1308/$01.00. Paper No. 20079.
Raudkivi, A.J. (1990): Loose boundary hydraulics, Third Edition, Pergamon Press, Great Britain.
Roberts, J., Jepsen, J., Gotthard, D., and Lick, W. (1998): Effects of particle size and bulk density on erosion of quartz particles, J. Hyd. Eng., ASCE, 124(12), pp. 1261–1267.
Sekine, M. and Iizuka N. (2000): Erosion rate of cohesive sediment, Korea Water Resources Association, ICHE, 4th International Conference on Hydro-Science and Engineering.
Takebayashi H., Luu Xian Loc, Egashira S., Tsukawaki S., Sim I., Sambath T., Sotham S., and Ide S. (2005): Flow pattern and size distribution of bed material at Chaktomuk in Cambodia, First International Symposium on Evaluation of Mechanisms Sustaining the Biodiversity in Lake Tonle Sap, Cambodia.

粘着性材料の非粘着性材料による侵食特性

ハルサント　プジ・グエン　マン　ミン　トアン*・竹林　洋史・藤田　正治

* 京都大学大学院　工学研究科

要　旨

本研究は非粘着性材料および水流による粘着性材料の侵食特性を明らかにするために行った。河床せん断力について議論するため，水路模型を用いた実験を行った。実験は粘着性材料を敷き詰めた水路上に非粘着性材料を供給するというものである。非粘着性材料の給砂量は平衡掃流砂量の0%～150%の範囲で与えた。実験の結果，河床が粘着性材料で構成されている場合，給砂する方が給砂しない場合よりも河床低下量が大きく，また侵食速度は掃流砂量の増加に伴って減少することが分かった。これは河床せん断力が流砂量の増加に伴って減少するためである。

キーワード: 粘着性材料，侵食速度，給砂量，非粘着性材料，せん断力